Future Foods 7 (2023) 100222

Contents lists available at ScienceDirect

Future Foods

journal homepage: www.elsevier.com/locate/fufo

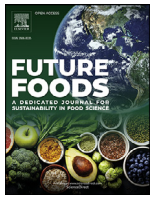

Research paper

Encapsulation of oil in the high moisture extrusion of wheat gluten: Interrelation between process parameters, matrix viscosity and oil droplet size

Christina Opaluwa[a,*], Tobias Lott[a], Heike P. Karbstein[a], M. Azad Emin[a,b]

[a] Food Process Engineering, Institute of Process Engineering in Life Sciences Karlsruhe Institute of Technology, Karlsruhe 76131, Germany
[b] Nexnoa GmbH, Aachener Str. 1042A, Köln 50858, Germany

ARTICLE INFO

Keywords:
Meat substitute
High moisture extrusion
Screw configuration
Wheat gluten
Oil addition
Viscosity

ABSTRACT

In plant protein-based meat substitutes, such as wheat gluten, oil is often added with the aim of improving sensory properties, like juiciness. When oil is added directly in the high moisture extrusion process, it must be homogeneously distributed and finely dispersed in the protein matrix to ensure both a stable process and a high quality of the final product. To gain a better understanding of droplet formation during the extrusion process, we investigate the relationship between process parameters, material properties and oil droplet size. We showed that at all oil contents, the use of reverse transport elements (RTE) prior to oil addition results in smaller oil droplets compared to forward transport elements. We attributed this to the fact that RTE increases the material temperature and residence time in the extruder and hence the viscosity of the protein matrix, which results from increased polymerization of the wheat gluten. The increased viscosity of the matrix can cause both an enhanced droplet breakup and a reduced coalescence of the droplets. However, with increasing the oil content from 1% to 4%, we noticed a remarkable increase in droplet size, independent of the matrix viscosity, which indicates the occurrence of coalescence.

1. Introduction

In recent years, concerns about ecological, ethical and health issues have led to a change in consumer behavior. A growing number of consumers are giving up meat products and products of animal origin. Instead, alternative products that replace animal proteins with plant proteins are becoming increasingly popular. These include cheese, milk, and yogurt alternatives, as well as meat substitutes that mimic meat in appearance, taste, and color (Elzerman et al., 2013; Hathwar et al., 2012; Kumar et al., 2017; Kyriakopoulou et al., 2021). A widely used process for the production of such meat substitutes is the high moisture extrusion with an attached cooling die. Here, the plant proteins are mixed with water, heated, and sheared by two co-rotating screws (Jia et al., 2020; Samard et al., 2019; Schmid et al., 2022; Wang et al., 2022; Zhang et al., 2018). During extrusion processing, the proteins form a multiphase system due to thermodynamic incompatibility between different protein fractions and protein conformations (native/denatured) (Cornet et al., 2022; Tolstoguzov, 1993; Wittek et al., 2021b). After the screw section, the material is pushed through a cooling die, where the material is cooled and solidified. The deformation of the multiphase system along the flow direction results in the formation of anisotropic product structures that are intended to resemble the muscle fibers of real meat (Akdogan, 1999; Cheftel et al., 1992; Osen and Schweiggert-Weisz, 2016; Wittek et al., 2021a).

In addition to muscle fibers, meat consists of inter- and intramuscular fat. The fat content in meat can vary greatly depending on the variety and origin and can account for up to 30% in total (Frank et al., 2016; Hocquette et al., 2010; Moloney and Teagasc, 2002). The intramuscular fat influences the tenderness and juiciness of the meat and thus has a great impact on the overall sensory quality of the meat (Choi et al., 2019; Egbert and Borders, 2006; Hoek et al., 2011b, 2011a). However, meat substitutes made from plant proteins often do not adequately reflect the sensory properties of meat. In fact, meat substitutes are often described as dry and poor in mouthfeel compared to real meat (Kumar and Kumar, 2011; Sadler, 2004). Therefore, plant fats or oils are added in order to improve sensory characteristics by increasing the juiciness and tenderness of the product (Egbert and Borders, 2006; Singh et al., 2021). Since the extrusion process can be flexibly adapted via numerous machine and process parameters, different processing steps can be combined in just one integrated processing step. This allows oil to be added directly into the extruder without the need for a previous emulsification step. Previous studies have shown for the extrusion of both starch

* Corresponding author.
E-mail address: christina.opaluwa@kit.edu (C. Opaluwa).

https://doi.org/10.1016/j.fufo.2023.100222
Received 15 October 2022; Received in revised form 27 February 2023; Accepted 11 March 2023

based (Emin et al., 2012a; Yılmaz et al., 2001) as well as protein based food products (Gwiazda et al., 1987; Kendler et al., 2021) that oil added in the extrusion process gets dispersed into droplets of different sizes. For laminar flow, which is predominant in extruders, shear and elongational stresses occur due to the rotation of the screws. The maximum shear rates and shear stresses are generated between the tip of the screw and the barrel wall, being responsible for a breakup of the oil phase into smaller droplets (Emin and Schuchmann, 2013a).

To describe the deformation and breakup of droplets in a laminar flow, dimensionless numbers are often used. The capillary number is defined as the ratio between the deforming viscous stresses and the shape-retaining interfacial stresses. The critical capillary number indicates the droplet diameter that can no longer be broken up in a given flow field (Taylor, 1932). For Newtonian systems, it was shown that the critical capillary number is a function of the viscosity ratio of dispersed phase to continuous matrix (Bentley and Leal, 1986; Grace, 1982). Emin et al. (2012b) found the same correlation for oil in plasticized starch matrix in simple shear flow. Nevertheless, due to the high viscosity of the starch matrix, the absolute values of the critical capillary number are up to 100 times lower than in Newtonian systems, which facilitates the break-up of the oil droplets. However, oil droplets may not only break up but also coalesce when being transported through the extruder (Utracki and Shi, 1992). The prerequisite for flow-induced coalescence is that at least two oil droplets collide and the film between the two droplets drains during their contact time. Film drainage is reduced at high matrix viscosities (Chesters, 1991). As stress is applied, breakup and coalescence can form a dynamic equilibrium, where the (equilibrium) droplet size distribution is time-independent. By coalescing, the size of the oil droplets increases until a critical droplet size is exceeded, and the droplet becomes unstable and breaks up again. Coalescence can be enhanced by the same factors that favor droplet breakup, which makes it difficult to differentiate between them. Factors that affect the competition between droplet breakup and flow-induced droplet coalescence are, e.g. collision probability, volume fraction of the dispersed phase, shear stresses and matrix viscosity and elasticity (Chesters, 1991; Elmendorp and van der Vegt, 1986; Janssen, 1993; Leal, 2004; Roland and Böuhm, 1984; Utracki and Shi, 1992). Oil droplet formation in protein matrices, which show the same viscoelastic behavior as polymer blends, has hardly been studied so far. The mechanisms of droplet breakup and coalescence in polymer blends are described in more detail in the recent review of Fortelný and Jůza (2019).

In meat substitute applications, plant proteins from various sources are used (Schmid et al., 2022; Singh et al., 2021; Wittek et al., 2021a; Guyony et al., 2022). Several plant proteins used on the market, e.g. wheat gluten, are highly reactive and undergo denaturation reactions due to thermomechanical treatment in the extruder (Akdogan et al., 1997; Arêas, 1992; Cheftel et al., 1992; Liu and Hsieh, 2008; Noguchi, 1989). Commercial wheat gluten, which we used in this study, is produced by a mechanical separation of wheat flour followed by a mild drying step at low temperatures. The gluten molecules are therefore in their native, folded conformation, which is stabilized mainly by non-covalent bonds that are sensitive to thermal treatment (Day et al., 2006). Upon heating, these bonds are disrupted and the wheat gluten molecule unfolds, exposing functional groups that were previously hidden inside the folded protein. New intermolecular bonds are formed between the exposed functional groups, leading to an irreversible aggregation. In wheat gluten, aggregation is dominated by the formation of covalent disulfide bonds (Schofield et al., 1983; Weegels et al., 1994). As a result, a three-dimensional protein network is formed and viscosity increases significantly (Emin et al., 2017). It has been reported for the high moisture extrusion of wheat gluten that the aggregation of wheat gluten via disulfide bonds is highly influenced by the material temperature, which in turn depends on various process parameters such as screw speed and screw configuration (Pietsch et al., 2017; Jia et al., 2020). Therefore, if oil is added during the extrusion process, it must be taken into account that, depending on the process parameters, the rheological properties of the wheat gluten change during the extrusion process, and thus also the stresses acting on the added oil phase along the screw and die section of the extruder. This makes the understanding of oil droplet formation during extrusion processing quite complex.

The objective of this study is to gain a better understanding of the relationship between the process parameters, rheological properties and final oil droplet size during the high moisture extrusion of wheat gluten. To decouple effects of viscosity changes due to wheat polymerization from viscosity-dependent competition between the breakup and coalescence of oil droplets, we chose an extrusion setup that allowed us to create two different processing zones in the extruder barrel by adjusting the screw configuration. In the first zone, the thermomechanical energy input was changed by altering the screw elements (forward/reverse) to obtain different wheat gluten viscosities. In the second zone, the oil was added and mixed into the wheat gluten matrix, so that the effect of protein matrix viscosity on oil droplet size could be investigated.

2. Materials and methods

2.1. Materials

Kröner Stärke (Ibbenbüren, Germany) kindly supplied vital wheat gluten, which is referred to as “gluten” throughout this paper. It contains 83% protein on dry matter basis according to the manufacturer’s specifications. Medium-chain triglycerides oil (MCT oil, WITARIX®60/40), which was purchased from IOI Oleo GmbH (Hamburg, Germany), is referred to as “oil” throughout this paper. The oil was stained at a concentration of 0.02 g/l with the lipophilic fluorescent dye nile red, purchased from Carl Roth (Karlsruhe, Germany).

2.2. Extrusion processing

The extrusion trials were carried out in a ZSK 26 Mc co-rotating twin screw extruder (Coperion, Stuttgart, Germany) with a screw diameter of 25.5 mm and a length-to-diameter (L/D) ratio of 29. The extruder barrel consists of seven barrel segments which, with the exception of the first segment, can be heated and cooled separately. The temperature profile was set to 40/80/120/120/120/120 °C in the barrel segments 2/3/4/5/6/7. The gluten was added into the first barrel segment by a gravimetrically controlled DDW-DDSR40 feeder (Brabender, Duisburg, Germany). A piston membrane pump (model KM 251, Alldos, Pfinztal, Germany) was used to pump water into the second barrel segment. The oil stained with nile red was added into the sixth barrel element using an HD 2–200 HPLC pump (Besta-Technik GmbH, Wilhelmsfeld, Germany). As the oil content (0, 1, 2, 4, 6%) increased, the water-to-gluten ratio was kept constant at 1:1, resulting in water contents of 51–52%. The total mass flow rate was constantly set to 10 kg/h. The extrusion experiments were performed applying screw speeds of 200, 400, 600, 800 and 1000 rpm.

The experimental set up is depicted in Fig. 1. By adjusting the barrel temperature and screw configuration, different processing zones were

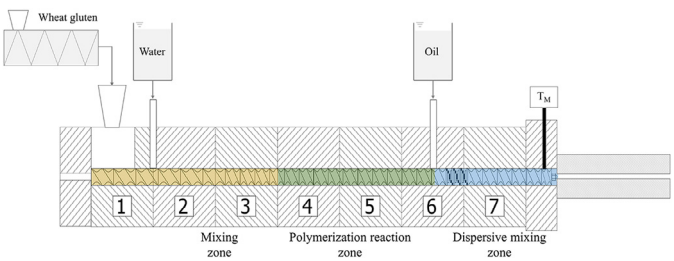

Fig. 1. Experimental set-up of extrusion trials. Mixing zone (yellow), polymerization reaction zone (green), dispersive mixing zone (blue).

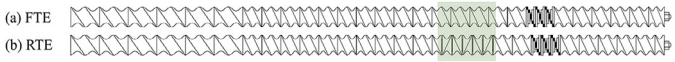

Fig. 2. Schematic illustration of the screw configurations used. (a) Forward transport elements (FTE) and (b) reverse transport elements (RTE) in the polymerization reaction zone. Differences in the screw configuration are highlighted in green.

generated along the extruder barrel: the mixing zone (barrel segment 2–3, yellow), where gluten and water are mixed at mild temperatures (40–80 °C), is followed by the polymerization reaction zone (barrel segment 4–6, green), where the barrel temperature is increased to 120 °C and thus the polymerization of gluten starts. In barrel segment 6, the oil is added into the dispersive mixing zone at 120 °C (barrel segment 6–7, blue), in which the oil phase is dispersed into the polymerized gluten matrix.

The screw configurations are shown in Fig. 2. Both configurations differ only in their design in the polymerization reaction zone, which is highlighted in green. The screw configuration (a) consists of forward transport elements (FTE) in the mixing as well as the polymerization reaction zone and of three forward kneading blocks in the dispersive mixing zone. The configuration (a) is referred to as “FTE” throughout the paper. Screw configuration (b) consists of forward transport elements in the mixing zone. In the polymerization reaction zone, three reverse transport elements (RTE) are incorporated to influence the polymerization reactions of the gluten. In the dispersive mixing zone, the configuration does not differ, it also contains of three forward kneading blocks. The configuration (b) is referred to as “RTE” throughout the paper.

The material temperature (T_M) and the process pressure (p) at the end of the extruder as well as the torque were recorded to characterize the process conditions. A rectangular cooling die with the dimensions 380 × 30 × 9 mm (l × w × h) was mounted at the end of the extruder barrel and cooled to 40 °C with a refrigeration unit (Presto Plus LH 47, Julabo GmbH, Seelbach, Germany). For the experiments without cooling die, a circular die with a diameter of 3 mm and a length of 25 mm replaced the cooling die. In the experiments with circular die, the temperature of the barrel segments 6–7 was adjusted so that T_M and p corresponded to the processing conditions with cooling die.

After the process conditions were stable for at least three minutes, samples were taken. In order to evaluate the anisotropic structures of the samples produced with cooling die, they were cut along the flow direction and opened relative to the flow direction, immediately after sampling. Images of the torn samples were taken with a digital camera (DMC-GH2, Lumix, Kadoma, Japan) at a resolution of 4608 × 3456 pixels. Additional samples were stored in airtight plastic bags at −18 °C until further investigation.

2.3. Determination of residence time distributions

The residence time distributions were measured by adding 0.3 g of carmine tracer to the first barrel segment and determining the time until the tracer discharged, according to Hirth et al. (2014). For this, the extrudate strand was filmed at the end of the cooling die and the color changes (a* values) were analyzed using MATLAB. For evaluation, the time of the first tracer exit, which is briefly referred to as "residence time", was determined. The residence time distributions were measured in triplicate.

2.4. Measurement of the complex viscosity

Rheological measurements of the samples were performed using an oscillatory closed cavity rheometer (RPA elite, TA Instruments, New Castle, Delaware, USA), its function is described in more detail in Wittek et al. (2020). For sample preparation, extrudate samples were pre-dried, milled to a particle size < 500 µm, dried to mass consistency, then re-hydrated in a Thermomix (Vorwerk, Wuppertal, Germany) to the original moisture content of the extrusion. This ensured that the water loss that can occur while sampling the hot extrudate samples is compensated and that all samples are adjusted to the same water content. Before the rheological measurements, the re-hydrated samples were vacuum packed and stored at 6 °C for at least 12 h to assure homogeneous water distribution.

For the measurements, 5.5 g of the sample was placed in the test chamber between two opposing cones. The two geometries are temperature-controlled and grooved to prevent slippage. The cavity is sealed and pressurized to 0.6 MPa in order to prevent water evaporation during measurement. As the lower cone oscillates at a defined frequency and strain amplitude, the torque response is recorded. From this, the rheological properties such as the complex viscosity can be calculated. For evaluating the influence of the process conditions on the material properties, frequency sweeps were performed at a temperature of 30 °C, in order to prevent the gluten from further polymerization reactions. The measurements were carried out in triplicate and conducted in a frequency range of 1–50 Hz within the linear viscoelastic range at a constant strain amplitude of 5%. To compare different samples, the complex viscosity $|\eta^*|$ at a constant frequency of 10.4 Hz was taken from the frequency sweeps and plotted.

2.5. Determination of the oil droplet size via CLSM

To investigate the influence of process conditions and material properties on the oil droplet size in the samples, the oil droplets were visualized by confocal laser scanning microscopy (CLSM). The oil was stained with the fluorescent dye nile red before extrusion processing, the protein matrix is autofluorescent. For the investigations via CLSM, the samples were cut using a CM 3050 cryo-microtome (Leica Biosystems GmbH, Nussloch, Germany). Small pieces of the samples (20 × 9 × 9 mm) were embedded in FSC 22 Blue Frozen Section Medium (Leica Biosystems GmbH, Nussloch, Germany) at −17 °C and cut into 40 µm thick slices in the cryo-microtome. After cutting, the slices were placed on microscope slides, dried at 55 °C and fixated with Mowiol (Carl Roth, Karlsruhe, Germany) and a cover slide. Per sample, three slices were taken.

A 63x Plan-Apochromat/1.4 oil DIC immersion objective was used to analyze the cryo-microtome slices in the CLSM (LSM 510 META, Carl Zeiss Microscope Systems, Jena, Germany). A 488 nm wavelength was used to excite the samples with an argon laser. To distinguish the signal of the stained oil from the protein signal, the emitted light was filtered with two different channels (oil: 575–615 nm, protein: 420–515 nm). For each of the three slices, at least 10 images were taken, so that a total of 30 images per sample were evaluated. MATLAB was used for image analysis and an area-weighted cumulative droplet size distribution (Q_2) was plotted from the obtained oil droplet areas. For each sample, the mean values and standard deviations were calculated from the size distributions of the individual slices.

3. Results and discussion

3.1. Formation of anisotropic structures

To evaluate if high moisture extrusion of wheat gluten with different oil contents produces anisotropic product structures for the two screw configurations used in this study, the extrudates were torn relative to the flow direction directly after extrusion processing. Fig. 3 shows images of samples with different oil contents for the screw configuration with only forward transport elements (FTE) and for the configuration with additional reverse transport elements (RTE). Comparing samples with increasing oil content, it can be clearly seen that for both FTE and RTE the anisotropic structures are less pronounced with increasing oil content. Especially in the case of FTE, it is apparent that the sample with 6% oil looks rather doughy and has hardly any defined structure, while the samples without oil have a structure that is clearly aligned

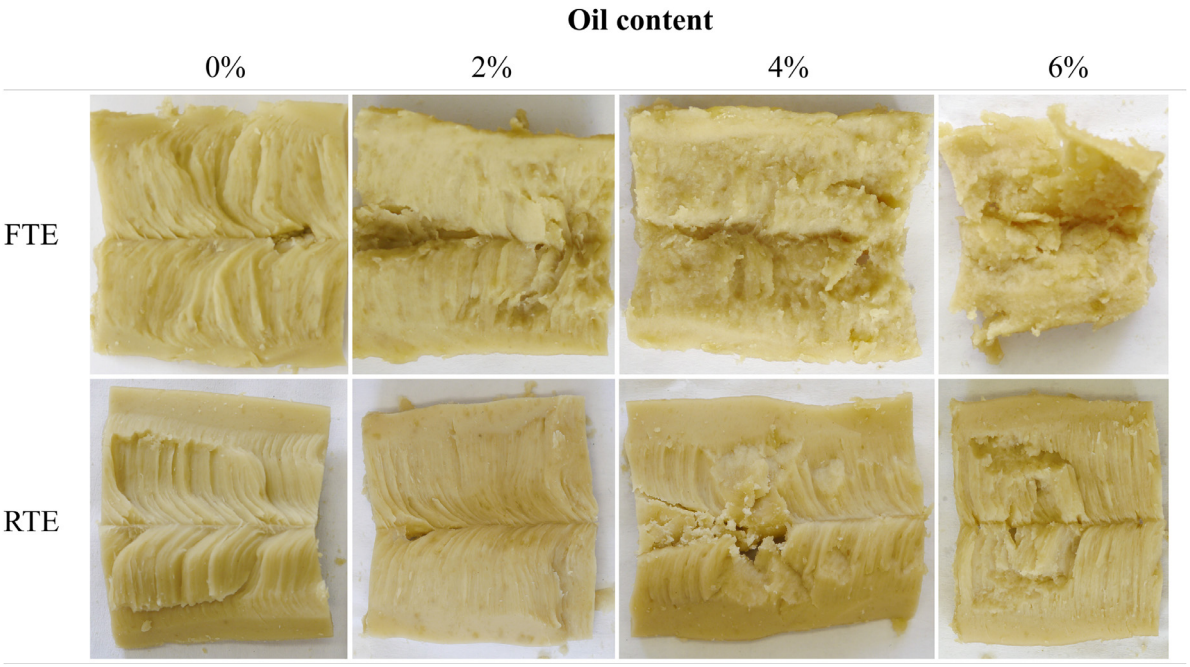

Fig. 3. Images of extrudate samples torn immediately after extrusion processing. Influence of reverse transport elements (RTE) in the polymerization reaction zone on the anisotropic structure as function of the oil content.

along the flow profile prevailing in the cooling die. This correlation between oil content and anisotropic structures has already been reported in literature (Gwiazda et al., 1987; Kendler et al., 2021).

A comparison of the samples extruded with the two different screw configurations (FTE and RTE, respectively, in the polymerization zone) shows that the anisotropic structures are more pronounced with RTE than with FTE, independent of the amount of oil added after wheat gluten polymerization. In particular, for the samples with 6% oil, it is noticeable that a weakly pronounced flow profile is still apparent when RTE is used, whereas no flow profile is apparent with FTE. In general, the differences in anisotropic structures are considered to depend mainly on die geometry, cooling temperature, mass flow rate, and rheological properties (Akdogan, 1999; Noguchi, 1989). Since the die geometry, cooling temperature, and mass flow rate were not changed, the differences between RTE and FTE samples are expected to be due to different rheological properties. The rheological properties of the protein matrix influence not only the formation of the anisotropic product structures, but also the formation of the oil droplets dispersed in the protein matrix. Therefore, the following section will address the influence of the screw configuration on process conditions and resulting rheological properties of the wheat gluten matrix.

3.2. Influence of screw configuration on process conditions and resulting properties of the matrix material

In Fig. 4(a) the material temperature at the end of the extruder barrel as a function of screw speed is depicted for the screw configurations FTE and RTE. As the screw speed increases from 200 rpm to 1000 rpm, the material temperature increases for both screw configurations. An increase of about 10 K is observed for the FTE configuration, and about 15 K for the RTE configuration. As an increase in screw speed intensifies mixing and increases the shear rates (Emin and Schuchmann, 2013a), the mechanical energy input into the gluten matrix is increased. This leads to an increase in material temperature due to viscous dissipation. The same correlation between screw speed and material temperature was found in several studies (Emin et al., 2021; Kendler et al., 2021; Palanisamy et al., 2019; Pietsch et al., 2019b).

Also, it can be seen that the use of RTE in the polymerization reaction zone leads to higher material temperatures at all screw speeds. For example, at a screw speed of 800 rpm, the use of RTE leads to a temperature increase of about 12 K compared to FTE. This can be attributed to the fact that reverse elements restrict the material flow, so that more material is subjected to high shear regions in this zone (Emin and Schuchmann, 2013a; Gogoi et al., 1996). Pietsch et al. (2017) also investigated the influence of reverse transport elements on the process conditions for the high moisture extrusion of gluten. They reported that the use of RTE leads to an increase in specific mechanical energy input, resulting in an increase in material temperature, which is in accordance to our results.

Fig. 4(b) shows the effect of the screw speed on the residence time of the gluten matrix in the extruder barrel for both screw configurations. A slight decrease in residence time is observed with increasing screw speed. This correlation is well known from literature (Choudhury and Gautam, 1998; Ganjyal and Hanna, 2002; Pietsch et al., 2019a; Yeh et al., 1992) and attributed to the fact that at constant total mass flow, the material is discharged faster as the screw speed increases. Furthermore, it is apparent that at all screw speeds, the residence time of the RTE configuration is about 10–15 s longer than the residence time of the FTE configuration. Reverse elements transport against the direction of flow, which results in a local accumulation of the material and thus in an extension of the residence time in the extruder barrel. Similar tendencies have been reported in experimental (Choudhury and Gautam, 1998; Schmid et al., 2021) as well as numerical (Ruyck, 1997; Vergnes et al., 1992) studies with reverse transport or reverse kneading elements. Summarizing, the results confirm that both the material temperature and the residence time in the extruder are significantly increased when reverse transport elements are used. According to Pietsch et al. (2019b), this will have an effect on the polymerization of the gluten molecules and thus on the rheological properties of the material.

In order to quantify this effect, the complex viscosity of the samples collected was determined using a closed cavity rheometer. Fig. 5(a) shows the complex viscosity of samples containing 0% oil as a function of screw speed for both screw configurations, FTE and RTE, respectively. As expected, the use of reverse transport elements (RTE) leads to higher complex viscosities at all screw speeds, with complex viscosities being two to three times higher for the RTE screw configuration. This is a result

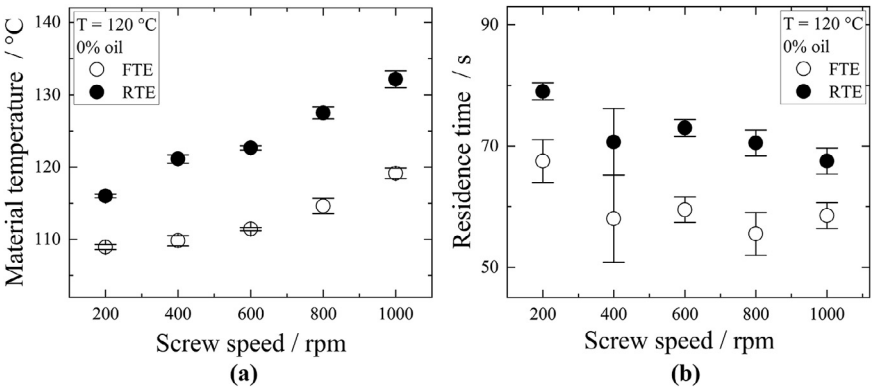

Fig. 4. (a) Material temperature and (b) residence time as a function of screw speed and screw configuration for samples without oil. Screw configuration with only forward transport elements (FTE) is shown by open symbols (○), with additional reverse transport elements (RTE) by filled symbols (●).

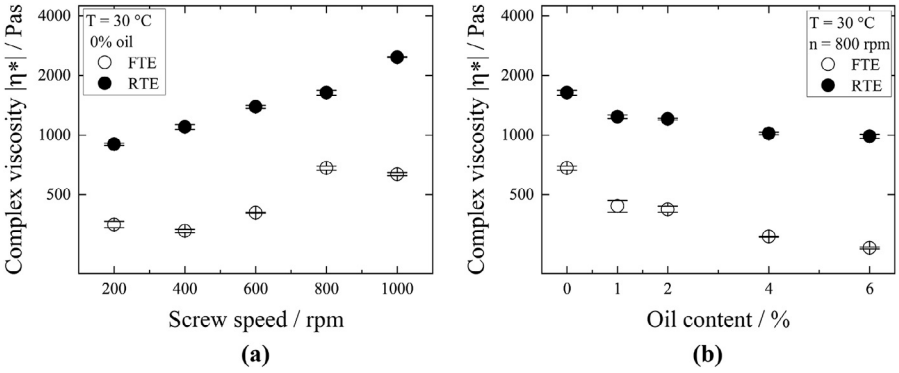

Fig. 5. Complex viscosity as a function of (a) screw speed for samples without oil and (b) oil content for samples containing 0–6% oil. Screw configuration with only forward transport elements (FTE) is shown by open symbols (○), with additional reverse transport elements (RTE) by filled symbols (●).

of higher material temperatures and longer residence times caused by the reverse element, leading to higher polymerization degrees and thus higher complex viscosities. For both screw configurations, an increase in complex viscosity is observed as screw speed increases from 200 rpm to 1000 rpm. According to the kinetic model of Pietsch et al. (2018) for wheat gluten polymerization under extrusion-like conditions, the thermal effect has a greater influence on the polymerization reactions than the time effect for extrusion-relevant residence times (> 90 s). Hence, when the screw speed is increased, the reduced residence time has less effect on polymerization than the increased material temperature, which explains why the complex viscosity increases with increasing screw speed.

To evaluate the influence of the oil addition on the material properties, the complex viscosities of samples with different oil contents (0–6%) were determined. Fig. 5(b) shows the complex viscosity as a function of oil content for both screw configurations, FTE and RTE, at a constant screw speed of 800 rpm. As expected, the use of reverse transport elements (RTE) results in higher complex viscosities than the use of forward transport elements (FTE) at all oil contents. Moreover, it can be seen that the addition of oil leads to a decrease in complex viscosity. For RTE, the addition of 4% oil leads to a reduction of the complex viscosity by about 30%, for FTE by about 50%. That the addition of oil leads to a decrease in matrix viscosity may have several reasons. On the one hand, the highly viscous protein matrix is diluted by the oil, on the other hand, oil could act as a plasticizer, leading to an additional increase in the molecular mobility of the wheat gluten molecules (Fu et al., 1997; Kendler et al., 2021).

3.3. Oil droplet size

In Fig. 6(a) and (b) CLSM images of samples with an oil content of 1% are depicted, using exemplarily the screw speed of $n = 800$ rpm. The autofluorescent gluten matrix appears in green, while the oil droplets appear in red. In both images it can be seen that the oil phase is homogeneously dispersed into droplets of small diameters. These observations match with results from previous studies (Gwiazda et al., 1987; Kendler et al., 2021). In Fig. 6(c) the corresponding cumulative size distributions are shown. It can be observed that when RTE is used, the curve is shifted to the left towards smaller droplet sizes compared to FTE.

The two screw configurations used do not differ in their geometry in the dispersive mixing zone, where the oil is added (see Fig. 2), resulting in exactly the same maximum shear rates. However, due to the different rheological properties of the matrix resulting from the use of RTE and FTE in the polymerization reaction zone, the shear stresses in the dispersive mixing zone are considerably different. This can affect both oil droplet breakup and coalescence. Higher complex viscosities of the matrix should increase the breakup of the oil droplets due to the higher shear stresses acting on them. At the same time, the probability of flow-induced coalescence is reduced because of the prolonged film drainage during droplet collisions. Due to both the increased oil droplet breakup and decreased coalescence, the dynamic equilibrium is expected to shift towards smaller oil droplet sizes when RTE are used in the polymerization reaction zone. In agreement with our observation, Emin et al. (2013b) found a decrease in droplet size at higher matrix viscosities in extruded starch matrices. Their results indicated that a higher matrix viscosity has no remarkable effect on breakup, but leads to a lower coalescence probability and thus to smaller oil droplets. This study may provide some hint that reduced coalescence due to higher matrix viscosity is the main mechanism leading to smaller droplet sizes.

Subsequently, the oil content was increased from 1% to 4%. Fig. 7 shows CLSM images of samples with 4% oil extruded with the (a) FTE and (b) RTE screw configurations at a screw speed of 800 rpm. The CLSM images were analyzed via image processing and area-weighted cumulative size distributions were generated (not shown). From the cumulative size distributions, the median droplet areas were taken and plotted against the oil content (1–4%) for both screw configurations, as shown in Fig. 7(c). Here, it becomes evident that the oil droplet size is smaller when using RTE than when using FTE at all oil contents. These

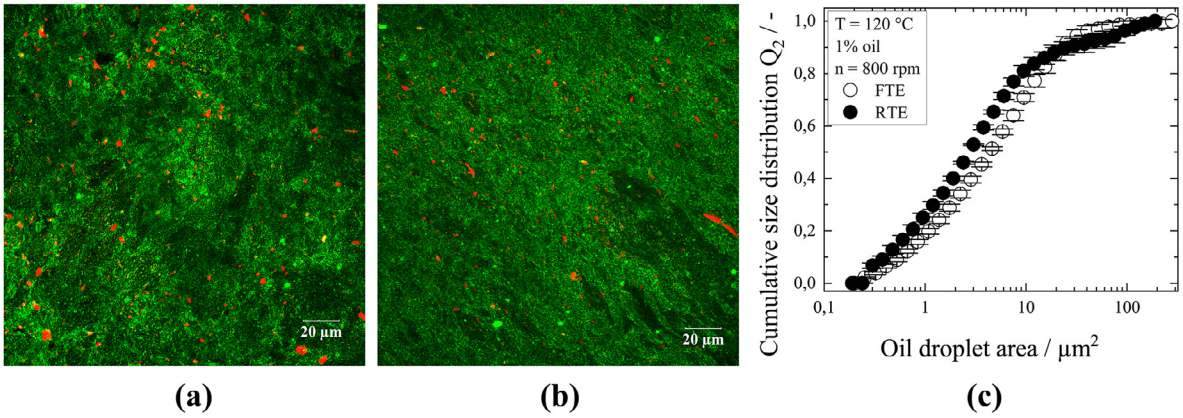

Fig. 6. Influence of the screw configuration on the oil droplet size. CLSM images of a samples with 1% oil extruded with the configuration (a) FTE and (b) RTE. (c) Oil droplet size distribution Q_2 for the samples depicted in (a) and (b). Screw configuration with only forward transport elements (FTE) is shown by open symbols (○), with additional reverse transport elements (RTE) by filled symbols (●).

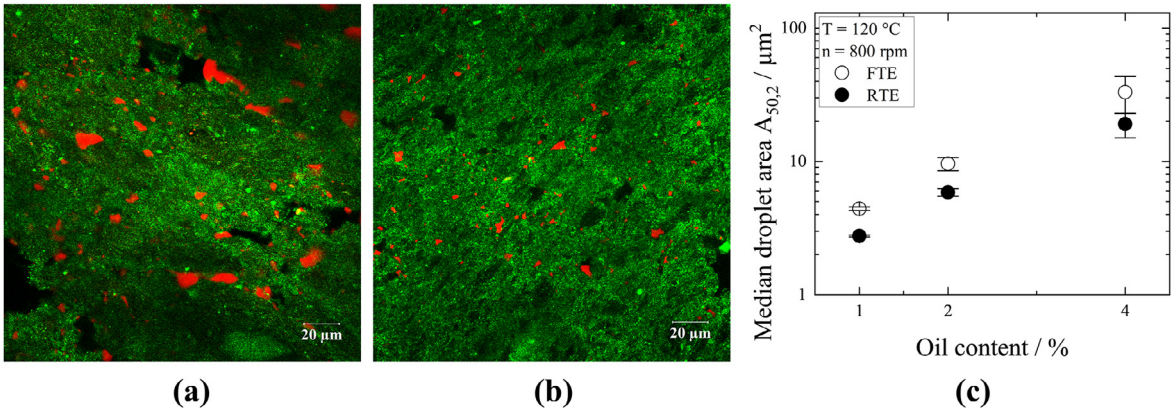

Fig. 7. Influence of the oil content on the oil droplet size for two different screw configurations. CLSM images of samples with 4% oil for (a) FTE configuration and (b) RTE configuration. (c) Median oil droplet area as a function of the oil content (1–4%) for RTE configuration (●) and FTE configuration (○).

results are in agreement with the results from Fig. 6, which were discussed in the previous section. Furthermore, it can be seen that with increasing oil content, the droplet size increases significantly for both screw configurations. For example, for RTE, increasing the oil content from 1% to 4% leads to an increase in droplet size by a factor of about 10. This may be due to both increased coalescence and decreased breakup. On the one hand, an increase in oil content leads to a significant increase in the number of oil droplets, which is expected to increase the flow-induced collision frequency and thus the coalescence probability (Chesters, 1991; Emin and Schuchmann, 2013b; Kendler et al., 2021). On the other hand, we have shown in the previous chapter that the matrix viscosity decreases with increasing oil content. Therefore, the shear stresses acting on the oil droplets can be expected to decrease, leading to less breakup of the oil droplets. Both increased coalescence and reduced breakup may contribute to a shift in oil droplet size towards larger oil droplets with increasing oil content.

3.4. *Influence of the attached cooling die on oil droplet size*

In the previous section, we suggest that the oil droplet size is formed in the dispersive mixing zone as a function of matrix viscosity, since matrix viscosity affects both, the droplet breakup as well as coalescence probability. The mixing efficiency through the rotation of the screws as well as the shear rates occurring in the dispersive mixing zone in the extruder barrel are remarkably higher than in the attached cooling die. Between the tips of the screw and the barrel wall local shear rates of up to 5000 s^{-1} can occur (Emin and Schuchmann, 2013a), while for the cooling die geometry and total mass flow used in this study we calculated apparent shear rates of only 6 s^{-1} according to Pahl et al. (1991). Due to the significantly lower shear rates, no further breakup of the oil droplets is to be expected in the cooling die. At the same time, the flow-induced coalescence of the oil droplets is expected to be significantly reduced in the cooling die, as the matrix viscosity increases due to its shear-thinning behavior as well as the temperature reduction. The size of the oil droplets formed in the dispersive mixing zone should therefore not change remarkably in the transition and cooling zone after the extruder barrel.

To evaluate this assumption, experiments were performed in which the long rectangular cooling die was replaced by a planar, non-cooled circular die. This setup is referred to as “without cooling die” throughout this section. Here, the process parameters (die diameter, die length and barrel temperature) were adjusted so that the process conditions, such as material temperature, were the same for both setups (Appendix, Fig. A1). This approach has already been successfully used in a previous study (Pietsch et al., 2017). It ensures that the gluten matrix experiences the same thermomechanical stresses in the extruder barrel. Hence, we assume that matrix viscosities in the extruder barrel are the same for both setups, resulting in comparable oil droplet sizes.

In Fig. 8, the mean oil droplet area is plotted against the oil content for samples extruded with and without cooling die, respectively, using the FTE configuration. The filled circle symbols correspond to the FTE-curve from Fig. 7. It can be seen from Fig. 8 that for both curves the oil droplet size increases with increasing oil content and that both curves are nearly on top of each other. This shows that the final droplet sizes

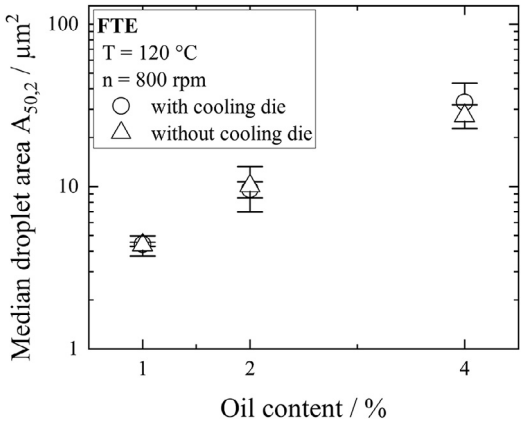

Fig. 8. Influence of the cooling die on the oil droplet size. Median oil droplet area as a function of the oil content for samples extruded with a rectangular cooling die (○) and without a cooling die (△) by using the FTE screw configuration.

of samples extruded with and without cooling die hardly differ from each other. The same trend could be observed for the RTE configuration (Appendix, Fig. A2).

We suggest therefore, that the oil droplet size is generated in the screw section and does not change significantly in the transition zone and along the cooling die, corresponding to the expectations drawn from the shear rates and temperatures in the dispersive mixing and cooling sections.

4. Conclusions

The dispersive mixing of oil during high moisture extrusion of wheat gluten for meat substitute applications was investigated in this study. Oil added directly in the high moisture extrusion process needs to be homogeneously distributed and finely dispersed in the protein matrix in order to achieve a stable process and high quality of the final product. To obtain more information about the oil droplet breakup and coalescence, we used two specific screw configurations (with/without reverse transport elements in the wheat gluten polymerization zone) that allowed adjustment of the matrix viscosity before oil addition. The influence of the screw configuration on the rheological properties of the gluten matrix as well as the oil droplet sizes in the extruded product were analyzed for different oil contents.

The use of reverse transport elements (RTE) in the polymerization reaction zone (before the oil addition point) increased the material residence time, material temperature, and matrix viscosity, which we attributed to an increased polymerization degree of the gluten. The images of the torn extrudates showed that the use of RTE resulted in more pronounced anisotropic structures, especially at higher oil contents. CLSM images of samples containing 1–4% oil revealed that the use of RTE resulted in smaller droplet sizes at all oil contents. Moreover, we observed an increase in the oil droplet size with increasing oil content, which can be attributed to both, an increased coalescence probability as well as a reduced oil droplet breakup due to decreased matrix viscosities. However, further research is needed to identify the underlying mechanisms in detail.

In summary, we demonstrated in this study that for polymerizing proteins such as wheat gluten, the matrix viscosity in the screw section can be adjusted by changing the screw configuration. We have also shown that increasing the viscosity of the matrix results in smaller oil droplets in the final product, which could be a potential strategy for further extrusion applications involving oil addition. However, since the oil droplet size increases with increasing oil content, regardless of the viscosity of the matrix, the amount of oil that can be added directly during extrusion is still limited.

Funding

This work was supported by the German Ministry of Economics and Climate Action (via AiF) and FEI (Forschungskreis der Ernährungsindustrie e.V., Bonn) in the scope of project AiF 20250N.

Declaration of Competing Interest

The authors declare no conflict of interest. The funders had no role in the design of the study; in the collection, analyses, or interpretation of data; in the writing of the manuscript, or in the decision to publish the results.

CRediT authorship contribution statement

Christina Opaluwa: Conceptualization, Data curation, Investigation, Methodology, Validation, Writing – original draft. **Tobias Lott:** Data curation, Investigation. **Heike P. Karbstein:** Resources, Writing – review & editing. **M. Azad Emin:** Conceptualization, Resources, Writing – review & editing.

Data availability

Data will be made available on request.

Acknowledgments

The authors would like to express their gratitude to Martin Bastmeyer, Marc Hippler and Lukas Lachenmaier from the Department of Cell- and Neurobiology, Zoological Institute, Karlsruhe Institute of Technology for supporting this work by enabling and supporting the CLSM Imaging and, to Benjamin Radel, Kerstin Sauther, Nina Weis and Jessica Wezstein for the experimental support.

Supplementary materials

Supplementary material associated with this article can be found, in the online version, at doi:10.1016/j.fufo.2023.100222.

References

Akdogan, H., 1999. High moisture food extrusion. Int. J. Food Sci. Technol. 34 (3), 195–207. doi:10.1046/j.1365-2621.1999.00256.x.

Akdogan, H., Tomás, R.L., Oliveira, J.C., 1997. Rheological properties of rice starch at high moisture contents during twin-screw extrusion. LWT Food Sci. Technol. 30 (5), 488–496. doi:10.1006/fstl.1996.0215.

Arêas, J.A., 1992. Extrusion of food proteins. Crit. Rev. Food Sci. Nutr. 32 (4), 365–392. doi:10.1080/10408399209527604.

Bentley, B.J., Leal, L.G., 1986. An experimental investigation of drop deformation and breakup in steady, two-dimensional linear flows. J. Fluid Mech. 167, 241–283. doi:10.1017/S0022112086002811.

Cheftel, J.C., Kitagawa, M., Queguiner, C., 1992. New protein texturization processes by extrusion cooking at high moisture levels. Food Rev. Int. 8 (2), 235–275. doi:10.1080/87559129209540940.

Chesters, A.K., 1991. Modelling of coalescence processes in fluid-liquid dispersions: a review of current understanding. Chem. Eng. Res. Des. 69 (A4), 259–270.

Choi, Y.M., Garcia, L.G., Lee, K., 2019. Correlations of sensory quality characteristics with intramuscular fat content and bundle characteristics in bovine longissimus thoracis muscle. Food Sci. Anim. Resour. 39 (2), 197–208. doi:10.5851/kosfa.2019.e15.

Choudhury, G.S., Gautam, A., 1998. On-line measurement of residence time distribution in a food extruder. J Food Sci. 63 (3), 529–534. doi:10.1111/j.1365-2621.1998.tb15779.x.

Cornet, S.H.V., Snel, SJ.E., Schreuders, F.K.G., van der Sman, R.G.M., Beyrer, M., van der Goot, A.J., 2022. Thermo-mechanical processing of plant proteins using shear cell and high-moisture extrusion cooking. Crit. Rev. Food Sci. Nutr. 62 (12), 3264–3280. doi:10.1080/10408398.2020.1864618.

Day, L., Augustin, M.A., Batey, I.L., Wrigley, C.W., 2006. Wheat-gluten uses and industry needs. Trends Food Sci. Technol. 17 (2), 82–90. doi:10.1016/j.tifs.2005.10.003.

Egbert, R., Borders, C., 2006. Achieving success with meat analogs. Food Technol. (60) 28–34. Online verfügbar unter https://agris.fao.org/agris-search/search.do?recordid=us201301056086 .

Elmendorp, J.J., van der Vegt, A.K., 1986. A study on polymer blending microrheology: part IV. The influence of coalescence on blend morphology origination. Polym. Eng. Sci. 26 (19), 1332–1338. doi:10.1002/pen.760261908.

Elzerman, JE., van Boekel, MA.J.S., Luning, P.A., 2013. Exploring meat substitutes: consumer experiences and contextual factors. Br. Food J. 115 (5), 700–710. doi:10.1108/00070701311331490.

Emin, M.A., Schmidt, U., van der Goot, A.J., Schuchmann, H.P., 2012a. Coalescence of oil droplets in plasticized starch matrix in simple shear flow. J. Food Eng. 113 (3), 453–460. doi:10.1016/j.jfoodeng.2012.06.015.

Emin, M.A., Schuchmann, H.P., 2013a. Analysis of the dispersive mixing efficiency in a twin-screw extrusion processing of starch based matrix. J. Food Eng. 115 (1), 132–143. doi:10.1016/j.jfoodeng.2012.10.008.

Emin, M.A., Schuchmann, H.P., 2013b. Droplet breakup and coalescence in a twin-screw extrusion processing of starch based matrix. J. Food Eng. 116 (1), 118–129. doi:10.1016/j.jfoodeng.2012.12.010.

Emin, M.A., Wittek, P., Schwegler, Y., 2021. Numerical analysis of thermal and mechanical stress profile during the extrusion processing of plasticized starch by non-isothermal flow simulation. J. Food Eng. 294, 110407. doi:10.1016/j.jfoodeng.2020.110407.

Emin, M.A, Mayer-Miebach, E., Schuchmann, H.P., 2012b. Retention of β-carotene as a model substance for lipophilic phytochemicals during extrusion cooking. LWT Food Sci. Technol. 48 (2), 302–307. doi:10.1016/j.lwt.2012.04.004.

Emin, M.A, Quevedo, M., Wilhelm, M., Karbstein, H.P., 2017. Analysis of the reaction behavior of highly concentrated plant proteins in extrusion-like conditions. Innov. Food Sci. Emerg. Technol. 44, 15–20. doi:10.1016/j.ifset.2017.09.013.

Fortelný, I., Jůza, J., 2019. Description of the droplet size evolution in flowing immiscible polymer blends. Polymers 11 (5). doi:10.3390/polym11050761, (Basel).

Frank, D., Joo, S.-.T., Warner, R., 2016. Consumer acceptability of intramuscular fat. Korean J. food Sci. Anim. Resour. 36 (6), 699–708. doi:10.5851/kosfa.2016.36.6.699.

Fu, J., Mulvaney, S.J., Cohen, C., 1997. Effect of added fat on the rheological properties of wheat flour doughs. Cereal Chem. 74 (3), 304–311. doi:10.1094/CCHEM.1997.74.3.304.

Ganjyal, G., Hanna, M., 2002. A review on residence time distribution (RTD) in food extruders and study on the potential of neural networks in RTD modeling. J. Food Sci. 67 (6), 1996–2002. doi:10.1111/j.1365-2621.2002.tb09491.x.

Gogoi, B.K., Choudhury, G.S., Oswalt, A.J., 1996. Effects of location and spacing of reverse screw and kneading element combination during twin-screw extrusion of starchy and proteinaceous blends. Food Res. Int. 29 (5/6), 505–512. doi:10.1016/S0963-9969(96)00051-8.

Grace, H.P., 1982. Dispersion phenomena in high viscosity immiscible fluid systems and applications of static mixers as dispersion device in such systems. Chem. Eng. Commun. 14 (3–6), 225–277. doi:10.1080/00986448208911047.

Guyony, V., Fayolle, F., Jury, V., 2022. High moisture extrusion of vegetable proteins for making fibrous meat analogs: a review. Food Rev. Int. 1–26. doi:10.1080/87559129.2021.2023816.

Gwiazda, S., Noguchi, A., Saio, K., 1987. Microstructural studies of texturized vegetable protein products: effects of oil addition and transformation of raw materials in various sections of a twin screw extruder. Food Struct. 6 (1), 57–61.

Hathwar, S.C., Rai, A.K., Modi, V.K., Narayan, B., 2012. Characteristics and consumer acceptance of healthier meat and meat product formulations-a review. J. Food Sci. Technol. 49 (6), 653–664. doi:10.1007/s13197-011-0476-z.

Hirth, M., Leiter, A., Beck, SM., Schuchmann, H.P., 2014. Effect of extrusion cooking process parameters on the retention of bilberry anthocyanins in starch based food. J. Food Eng. 125 (2), 139–146. doi:10.1016/j.jfoodeng.2013.10.034.

Hocquette, J.F., Gondret, F., Baéza, E., Médale, F., Jurie, C., Pethick, D.W., 2010. Intramuscular fat content in meat-producing animals: development, genetic and nutritional control, and identification of putative markers. Animal 4 (2), 303–319. doi:10.1017/S1751731109991091.

Hoek, A.C., Luning, P.A., Weijzen, P., Engels, W., Kok, F.J., Graaf, C., 2011a. Replacement of meat by meat substitutes. A survey on person- and product-related factors in consumer acceptance. Appetite 56 (3), 662–673. doi:10.1016/j.appet.2011.02.001.

Hoek, A.C., van Boekel, M.A.J.S., Voordouw, J., Luning, P.A., 2011b. Identification of new food alternatives: how do consumers categorize meat and meat substitutes? Food Qual. Prefer. 22 (4), 371–383. doi:10.1016/j.foodqual.2011.01.008.

Janssen, J.M.H., 1993. Dynamics of Liquid-Liquid Mixing. Technische Universiteit Eindhoven [Phd Thesis 1 (Research TU/e /Graduation TU/e), Chemical Engineering and Chemistry] doi:10.6100/IR404184.

Jia, F., Wang, J., Wang, Qi, Zhang, X., Chen, Di, Chen, Yu, Zhang, C., 2020. Effect of extrusion on the polymerization of wheat glutenin and changes in the gluten network. J. Food Sci. Technol. 57 (10), 3814–3822. doi:10.1007/s13197-020-04413-6.

Kendler, C., Duchardt, A., Karbstein, H.P., Emin, M.A., 2021. Effect of oil content and oil addition point on the extrusion processing of wheat gluten-based meat analogues. Foods 10 (4), 697. doi:10.3390/foods10040697.

Kumar, P., Chatli, M.K., Mehta, N., Singh, P., Malav, O.P., Verma, A.K., 2017. Meat analogues: health promising sustainable meat substitutes. Crit. Rev. Food Sci. Nutr. 57 (5), 923–932. doi:10.1080/10408398.2014.939739.

Kumar, P., Kumar, R.R., 2011. Product profile comparison of analogue meat nuggets versus chicken nuggets. Fleischwirtsch. Int. J. Meat Prod. Meat Process. 1, 72–74.

Kyriakopoulou, K., Keppler, J.K., van der Goot, A.J., Boom, R.M., 2021. Alternatives to meat and dairy. Annu. Rev. Food Sci. Technol. 12, 29–50. doi:10.1146/annurev-food-062520-101850.

Leal, L.G., 2004. Flow induced coalescence of drops in a viscous fluid. Phys. Fluids 16 (6), 1833–1851. doi:10.1063/1.1701892.

Liu, K.S., Hsieh, F.H., 2008. Protein-protein interactions during high-moisture extrusion for fibrous meat analogues and comparison of protein solubility methods using different solvent systems. J. Agric. Food Chem. 56 (8), 2681–2687. doi:10.1021/jf073343q.

Moloney, A.P., Teagasc, D., Kerry, J, Kerry, J., Ledward, D., 2002. The fat content of meat and meat products. In: (Hg.): Meat Processing: Improving Quality. Woodhead Publishing, pp. 137–153.

Noguchi, A., Mercier, C., Linko, P., Harper, J.M., 1989. Extrusion cooking of high-moisture protein foods. In: (Hg.): Extrusion cooking. Minnesota. AACC, pp. 343–369.

Osen, R., Schweiggert-Weisz, U., Smithers, G.W., 2016. High-moisture extrusion: meat analogues. In: (Hg.): Reference Module in Food Science. Elsevier, pp. 1–7.

Pahl, MH., Gleissle, W., Laun, H.M., 1991. Praktische Rheologie der Kunststoffe und Elastomere. VDI-Verlag, Düsseldorf.

Palanisamy, M., Franke, K., Berger, RG., Heinz, V., Töpfl, S., 2019. High moisture extrusion of lupin protein: influence of extrusion parameters on extruder responses and product properties. J. Sci. Food Agric. 99 (5), 2175–2185. doi:10.1002/jsfa.9410.

Pietsch, VL., Emin, M.A, Schuchmann, H.P., 2017. Process conditions influencing wheat gluten polymerization during high moisture extrusion of meat analog products. J Food Eng 198, 28–35. doi:10.1016/j.jfoodeng.2016.10.027.

Pietsch, VL., Karbstein, HP., Emin, M.A, 2018. Kinetics of wheat gluten polymerization at extrusion-like conditions relevant for the production of meat analog products. Food Hydrocoll. 85, 102–109. doi:10.1016/j.foodhyd.2018.07.008.

Pietsch, VL., Schöffel, F., Rädle, M., Karbstein, HP., Emin, M.A, 2019a. High moisture extrusion of wheat gluten: modeling of the polymerization behavior in the screw section of the extrusion process. J. Food Eng. 246, 67–74. doi:10.1016/j.jfoodeng.2018.10.031.

Pietsch, VL., Werner, R., Karbstein, HP., Emin, M.A, 2019b. High moisture extrusion of wheat gluten: relationship between process parameters, protein polymerization, and final product characteristics. J. Food Eng. 259, 3–11. doi:10.1016/j.jfoodeng.2019.04.006.

Roland, C.M., Böuhm, G.G.A., 1984. Shear-induced coalescence in two-phase polymeric systems. I. Determination from small-angle neutron scattering measurements. J. Polym. Sci. Polym. Phys. Ed. 22 (1), 79–93. doi:10.1002/pol.1984.180220108.

Ruyck, H., 1997. Modelling of the residence time distribution in a twin screw extruder. J. Food Eng. 32 (4), 375–390. doi:10.1016/S0260-8774(97)00012-5.

Sadler, MJ., 2004. Meat alternatives—market developments and health benefits. Trends Food Sci. Technol. 15 (5), 250–260. doi:10.1016/j.tifs.2003.09.003.

Samard, S., Gu, B.Y., Ryu, G.H., 2019. Effects of extrusion types, screw speed and addition of wheat gluten on physicochemical characteristics and cooking stability of meat analogues. J. Sci. Food Agric. 99 (11), 4922–4931. doi:10.1002/jsfa.9722.

Schmid, E.M., Farahnaky, A., Adhikari, B., Torley, P.J., 2022. High moisture extrusion cooking of meat analogs: a review of mechanisms of protein texturization. Compr. Rev. Food Sci. Food Saf. 00, 1–37. doi:10.1111/1541-4337.13030.

Schmid, V., Trabert, A., Keller, J.S., Bunzel, M., Karbstein, H.P., Emin, M.A., 2021. Functionalization of enzymatically treated apple pomace from juice production by extrusion processing. Foods 10 (3). doi:10.3390/foods10030485.

Schofield, J.D., Bottomley, R.C., Timms, M.F., Booth, M.R., 1983. The effect of heat on wheat gluten and the involvement of sulphydryl-disulphide interchange reactions. J. Cereal Sci. 1 (4), 241–253.

Singh, M., Trivedi, N., Enamala, M.K., Kuppam, C., Parikh, P., Nikolova, MP., Chavali, M., 2021. Plant-based meat analogue (PBMA) as a sustainable food: a concise review. Eur. Food Res. Technol. 247 (10), 2499–2526. doi:10.1007/s00217-021-03810-1.

Taylor, G.I., 1932. The viscosity of a fluid containing small drops of another fluid. Proc. R. Soc. Lond. Contain. Pap. Math. Phys. Character 138 (834), 41–48. doi:10.1098/rspa.1932.0169.

Tolstoguzov, V.B., 1993. Thermoplastic extrusion—The mechanism of the formation of extrudate structure and properties. J. Am. Oil Chem. Soc. 70 (4), 417–424. doi:10.1007/BF02552717.

Utracki, L.A., Shi, Z.H., 1992. Development of polymer blend morphology during compounding in a twin-screw extruder. part I: droplet dispersion and coalescence—a review. Polym. Eng.Sci. 32 (24), 1824–1833. doi:10.1002/pen.760322405.

Vergnes, B., Barrès, C., Tayeb, J., 1992. Computation of residence time and energy distributions in the reverse screw element of a twin-screw extrusion-cooker. J. Food Eng. 16 (3), 215–237. doi:10.1016/0260-8774(92)90035-5.

Wang, H., Zhang, L., Czaja, T.P., Bakalis, S., Zhang, W., Lametsch, R., 2022. Structural characteristics of high-moisture extrudates with oil-in-water emulsions. Food Res. Int. 158, 111554. doi:10.1016/j.foodres.2022.111554.

Weegels, P.L., de Groot, A.M.G., Verhoek, J.A., Hamer, R.J., 1994. Effects on gluten of heating at different moisture contents. II. Changes in physico-chemical properties and secondary structure. J. Cereal Sci. 19 (1), 39–47.

Wittek, P., Karbstein, HP., Emin, M.A, 2021a. Blending proteins in high moisture extrusion to design meat analogues: rheological properties, morphology development and product properties. Foods 10 (7). doi:10.3390/foods10071509.

Wittek, P., Zeiler, N., Karbstein, HP., Emin, M.A, 2020. Analysis of the complex rheological properties of highly concentrated proteins with a closed cavity rheometer. Appl. Rheol. 30 (1), 64–76. doi:10.1515/arh-2020-0107.

Wittek, P., Zeiler, N., Karbstein, HP., Emin, M.A, 2021b. High moisture extrusion of soy protein: investigations on the formation of anisotropic product structure. Foods 10 (1). doi:10.3390/foods10010102.

Yeh, A.I., Hwang, S.J., Guo, J.J., 1992. Effects of screw speed and feed rate on residence time distribution and axial mixing of wheat flour in a twin-screw extruder. J. Food Eng. 17 (1), 1–13. doi:10.1016/0260-8774(92)90061-A.

Yılmaz, G., Jongboom, R.O.J., Feil, H., Hennink, W.E., 2001. Encapsulation of sunflower oil in starch matrices via extrusion: effect of the interfacial properties and processing conditions on the formation of dispersed phase morphologies. Carbohydr. Polym. 45 (4), 403–410. doi:10.1016/S0144-8617(00)00264-2.

Zhang, J., Liu, Li, Liu, H., Yoon, A., Rizvi, S.S.H., Wang, Q., 2018. Changes in conformation and quality of vegetable protein during texturization process by extrusion. Crit. Rev. Food Sci. Nutr. 59 (20), 3267–3280. doi:10.1080/10408398.2018.1487383.